J Mater Sci (2009) 44:6505–6511
DOI 10.1007/s10853-009-3571-z

MESOSTRUCTURED MATERIALS

Crossed-discs of mesoporous silica SBA-15 and their carbon replicas

Feng Li · Jin-Gui Wang · Yu-Ping Liu · Hui-Jing Zhou · Tie-Hong Chen

Received: 16 October 2008 / Accepted: 12 May 2009 / Published online: 27 May 2009

Abstract Crossed-discs of mesoporous silica SBA-15 were synthesized by using tetramethylorthosilicate (TMOS) as silica source in the presence of Sn^{2+} cations. The silica crossed-discs were characterized by small-angle X-ray scattering (SAXS), scanning electron microscopy (SEM), transmission electron microscopy (TEM), and nitrogen adsorption. All the results show that the materials have hexagonally ordered channels running parallel to the thickness of the discs. The effects of the reaction conditions on the morphology of the materials were discussed. The SBA-15 crossed-discs were used as hard templatesto obtain their carbon replicas.

Introduction

Mesoporous silica materials [1–3] have attracted much attention due to their potentials in practical applications such as catalysis, separation, nanoreactors, and sensors. In 1998, mesoporous silica SBA-15 was invented by using amphiphilic triblock copolymer as the template [4]. SBA-15 has a hexagonal arrangement of cylindrical channels with diameters in the range of 2–30 nm, and when compared with MCM-41, SBA-15 has higher thermal stability, and relatively thicker silica walls, as well as some intrawall micropores. Because the morphologies of the mesoporous silica greatly influence their practical applications, extensive studies have been focused on morphological control of SBA-15, and the materials with various shapes have been prepared, such as fibers, ropes, spheres, rods, etc. [4–13].

Bao and coworkers synthesized cuboid-like SBA-15 with the channels running parallel to the short axis by using excess amount of decane [14]. Sujandi et al. reported on the amino-functionalized SBA-15 with a platelet morphology using aminopropyltriethoxysilane (APTES), and the channels were found to be parallel to the thickness of the platelets [15]. Besides the addition of oil or solvent, Somorjai's group reported on the fabrication of hyper-branched, network-like structure of SBA-15 with the addition of Cu^{2+} [16]. Recently, SBA-15 silica of platelet shape and very short mesochannels (150–350 nm) was synthesized by introducing Zr(IV) ions [17]. Herein, we report the synthesis of SBA-15 crossed-discs under a static condition by using tetramethylorthosilicate (TMOS) as silica source in the presence of Sn^{2+}. The hexagonally packed cylindrical mesopores were found to be parallel to the thickness of the discs, that is, all the mesoporous channels of SBA-15 were parallel to short axis of the disc. Such an orientation results in relatively short length of the nanoscale channels, which would be favorable for mass transfer [18]. It would be significant to note that the morphology of the crossed-discs will effectively prevent the particles from closely stacking in practical applications. With the use of the SBA-15 crossed-discs as templates, we also obtained their carbon replicas with both micro- and mesoporosities.

F. Li · J.-G. Wang · Y.-P. Liu · H.-J. Zhou · T.-H. Chen (✉)
Institute of New Catalytic Materials Science, Key Laboratory of Energy-Material Chemistry (Tianjin) and Engineering Research Center of Energy Storage & Conversion (MOE), College of Chemistry, Nankai University, Tianjin 300071, People's Republic of China
e-mail: chenth@nankai.edu.cn

Experimental

Materials

Tetramethylorthosilicate (TMOS, A.R.) was purchased from Wuhan University Silicone New Material Co., China, and Tetraethylorthosilicate (TEOS, A.R.) from Tianjin REGENT CHEMCALS Co., Ltd. $EO_{20}PO_{70}EO_{20}$ (P123 A.R.) was purchased from Nanjing Weier Co., China. $SnCl_2 \cdot 2H_2O$ (A.R.) was purchased from Yunnan Tin Co., China. All the materials were used as received without further purification.

Synthesis

The preparation procedure of the silica crossed-discs was as follows: 0.67 g $EO_{20}PO_{70}EO_{20}$ (P123) was dissolved in a solution of 5-mL deionized water and 20 mL of HCl (2.0 M), followed by addition of 0.09 g $SnCl_2 \cdot 2H_2O$. After 1 h stirring, 1.03 g TMOS was added to the solution. The final molar ratio of the reactants was P123:HCl:H_2O:$SnCl_2 \cdot 2H_2O$:TMOS = 0.017:5.91:194:0.059:1. The mixture was stirred for 15 s, kept under static conditions at 38 °C for 24 h, and transferred into a Teflon bottle at 80 °C for another 24 h. The solid product was collected by filtration, washed with deionized water, dried in air, and calcined at 550 °C for 5 h to remove the template. The SBA-15 cross-discs were used as templates to prepare mesoporous carbon as per the following procedure: 0.1 g of calcined SBA-15 product was added to a solution containing 0.1 g sucrose, 0.02 g H_2SO_4, and 5 g H_2O. The mixture was evacuated for 6 h at 100 °C and subsequently at 150 °C for 6 h. This treatment was repeated twice. The carbonization was completed by heating the specimen to 900 °C for 2 h under N_2 environment. Finally, the template silica wall was removed with HF solution [19].

Characterizations

Small-angle X-ray scattering (SAXS) experiments were performed on a Bruker Nanostar small angle X-ray scattering system. The plot of intensity versus scattering wave vector was produced by circularly averaging two-dimensional scattering patterns. N_2 adsorption measurements were performed at 77 K using a Quantachrome NOVA 2000e analyzer and a Tristar 3000 sorption analyzers. Before measurements, the sample was outgassed at 473 K for 4 h. The specific surface area was calculated by Multi-BET (Brunauer, Emmett and Teller) in the range of relative pressure 0.1–0.3. The pore size distribution (PSD) was calculated by Barret–Joyner–Halenda (BJH) method from adsorption branch. Scanning electron microscopy (SEM) observations were carried out on a Shimadzu SS-550 scanning electron microscope. Transmission electron microscopy (TEM) observations were carried out on a Philips Tecnai F20 transmission electron microscope working at 200 kV. XPS spectra were obtained with a Kratos Axis Ultra DLD instrument.

Results and discussion

The representative (SEM) images of the calcined product are shown in Fig. 1, where single-crystal-like particles with disc-like morphology can be seen. The size of the discs is around 3–4 μm in diameter and the thickness is about 200–350 nm, indicating a high aspect ratio of the discs. A distinct feature of the morphology is that most of the discs grow in pairs and crosswise, which would effectively prevent the particles from closely stacking. Disk-shaped ZnO complex microstructures has been reported recently [20]. From the TEM images (Fig. 1c, d), crossed-discs can be found, and under higher magnification, it can be clearly seen that well hexagonally ordered nanochannels are parallel to the thickness of the disc examined; thus, the individual SBA-15 discs can be regarded as single-domain particles. Figure 2a displays the SAXS pattern of the product. Three distinguished diffraction peaks at d spacings of 11.93, 6.79, and 5.85 nm are observed, corresponding to the (100), (110), and (200) diffractions, respectively, indicating a well-ordered two-dimensional hexagonal mesostructure. Figure 2b is the nitrogen adsorption–desorption isotherm, showing a type IV isotherm with H1-type hysteresis loop. The Brunauer–Emmett–Teller (BET) surface area of the product is 741 $m^2\ g^{-1}$, with a pore volume of 0.76 $cm^3\ g^{-1}$ and a narrow PSD centered at 9.9 nm calculated from the adsorption branch based on the BJH model (Fig. 2b, inset).

The morphologies of SBA-15 can be controlled by several factors, including temperature, hydrolysis, and condensation rate of silica sources, inorganic salts, the shearing force, as well as the complex interplay of these factors, according to the colloidal phase separation mechanism (CPSM) proposed by Yu et al. [21]. In this study, if TEOS was used as silica source instead of TMOS, then particles with diameters about 500 nm were obtained (Fig. 3a). The induction time for the formation of white precipitation was much longer than that taken when using TMOS, due to the relatively lower hydrolysis rate of the TEOS. When increasing the temperature to 45 °C, the induction time for the formation of white precipitation was shortened, and crossed-discs morphology of SBA-15 (Fig. 3b) could also be obtained. Therefore, the hydrolysis and condensation rate of the silica precursors would efficiently affect the morphology of the SBA-15 in our synthesis system. The hydrolysis and condensation rate of the

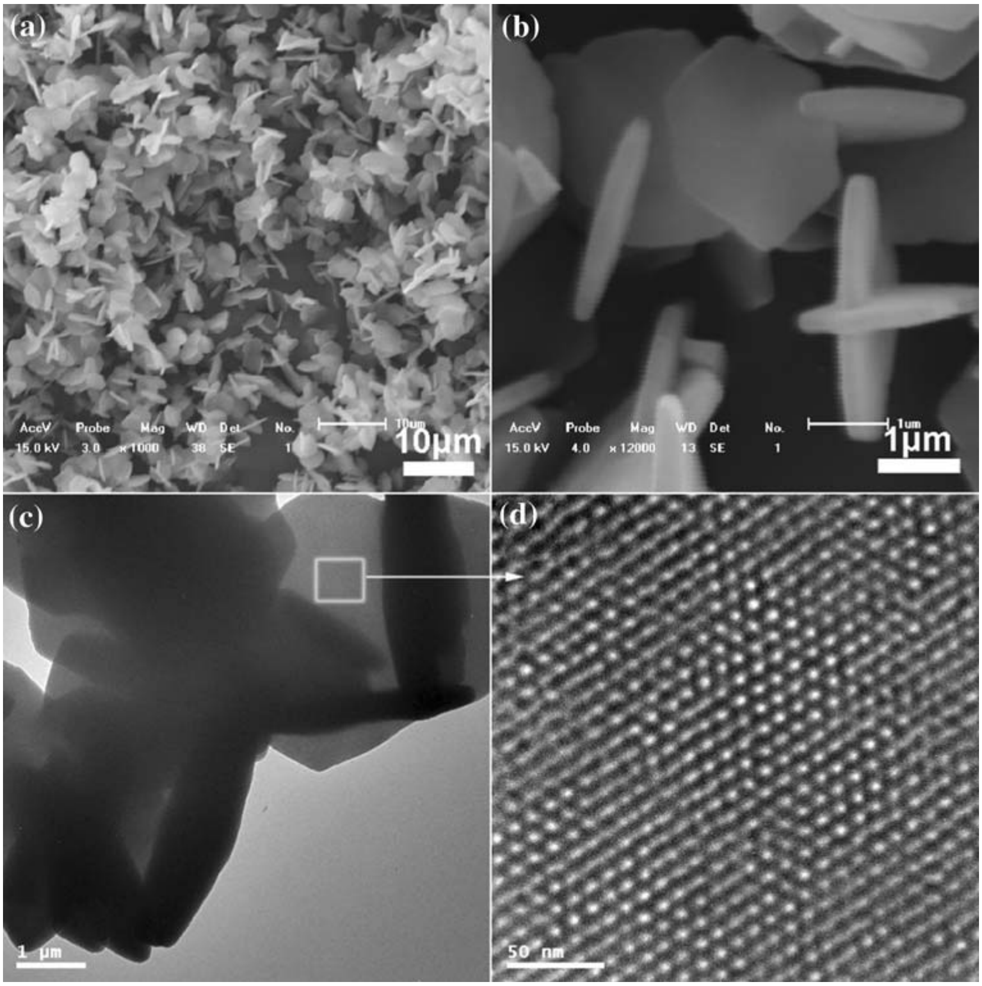

Fig. 1 Low magnification SEM (**a**, **b**) and TEM (**c**) images of the SBA-15 crossed-discs. **d** Higher magnification TEM image showing hexagonal arrangement the mesopores along the short axis of a disc-like particle

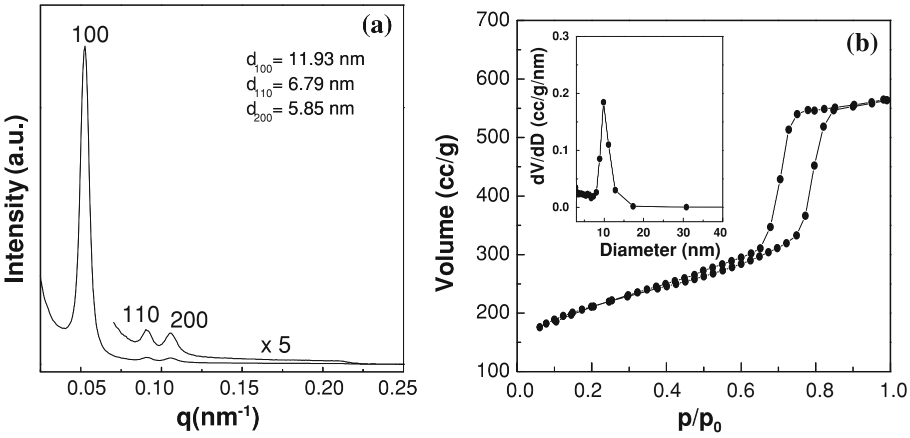

Fig. 2 **a** SAXS pattern of the sample and **b** the corresponding nitrogen adsorption–desorption isotherm and pore size distribution by BJH method (inset)

silica precursors would affect the rate of cooperative assembly of the silica and surfactant, which leads to the change of the morphology. In our experiments, SBA-15 crossed-discs with diameter 3–4 µm and thickness of 200–350 nm were already formed after 3 h of reaction (Fig. 3c). All the samples prepared at temperatures of 38 °C, 60 °C, 100 °C, and 130 °C, respectively, were composed of 100% crossed-discs-like particles (Fig. 4), indicating that the aging temperature did not affect much the morphologies of the product. A parallel synthesis was also performed under

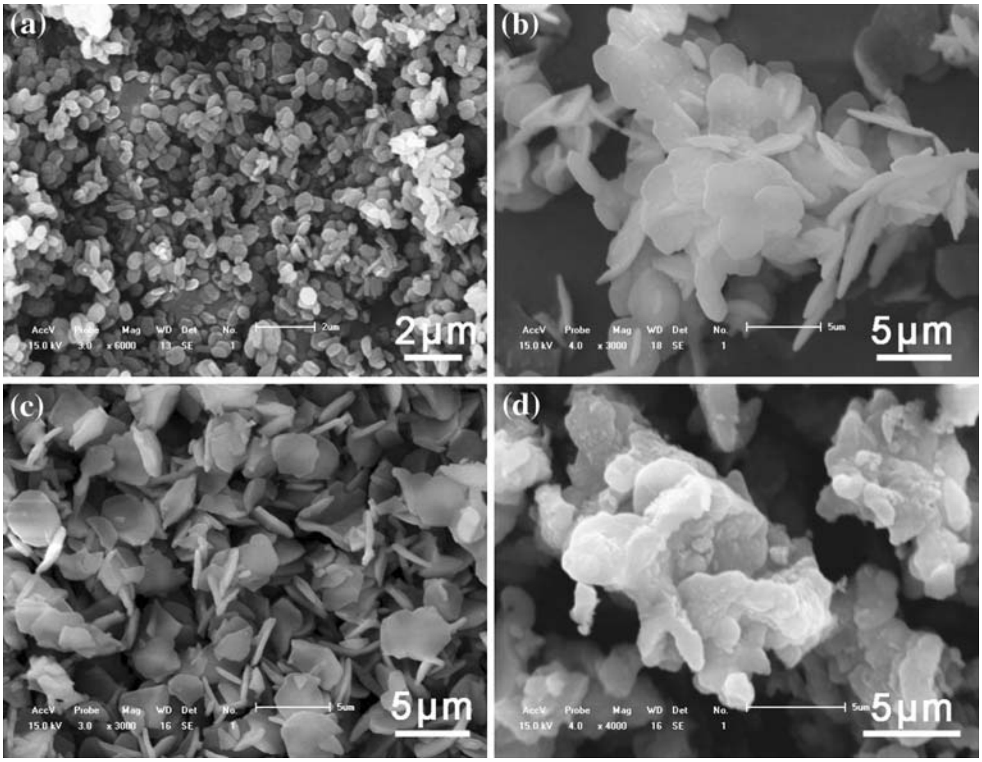

Fig. 3 SEM images of the as-synthesized products **a** prepared using TEOS at 38 °C, and **b** at 45 °C, **c** sample reacted for 3 h using TMOS at 38 °C, and **d** prepared under stirring during the reaction

stirring from the initial stage, and the morphology of the product became aggregated irregular particles (Fig. 3d).

If the synthesis was performed without the addition of Sn^{2+}, then hexagonal platelike SBA-15 particles were obtained, with the size of 2 μm in diameter and the thickness of about 800 nm (Fig. 5a), indicating a relatively low aspect ratio compared with the crossed-discs when synthesized in the presence of Sn^{2+}. These particles were severely aggregated, and some of them also grew in pairs, as indicated by the arrows in Fig. 5a. This indicates that the presence of Sn^{2+} is not necessary to induce the cross-growth of the SBA-15 particles. However, Sn^{2+} could be responsible for the formation of SBA-15 crossed-discs with relatively high aspect ratio under the quiescent condition at 38 °C and with TMOS as the silica source. The concentration of Sn^{2+} cations is also important. SBA-15 crossed-discs were obtained with the Sn/Si ratio between 1:50 and 3:50 (Fig. 5b, c). However, when Sn/Si ratio was increased to 5:50, only SBA-15 granules formed (Fig. 5d), probably because of the higher ionic strength which could affect the condensation rate of silica source in the solution. It has been reported that Sn^{4+} can be incorporated in the silica framework to form Sn-SBA-15 [22]. In this study, incorporation of Sn into the silica wall was difficult due to the addition of Sn^{2+}. The Sn-free silica wall was proved by XPS characterization of the sample (Fig. 6).

In order to study how these crossed particles grow from the solution, we performed time-dependent synthesis under the quiescent condition at 38 °C and with TMOS as silica source. A series of products obtained at different reaction times were examined by TEM. After 12 min of the reaction, milky-white solution appeared. The products, being too small to be filtered at this stage, were recovered by centrifugation. With cryo-TEM experiments of the SBA-15 synthesis solution as reported in some previous reports, thread-like micelles and hexagonally arranged micellar bundles have been detected [23]. From our own TEM image, bundles of micelle rods with short-range order were also observed, which coalesce together with different orientations (Fig. 7a). After 40 min of reaction, small crossed particles were detected (Fig. 7c, d). This implies that the crossed growth of the particles may originate from the nucleation stage.

According to Somorjai and coworkers [16], in the presence of metal cations, the synthesis pathway of SBA-15 could be $N^0[(M^{n+} + H^+)]X^-]I^+$, where M^{n+} represents the metal ions, which would have chelating interactions with the PEO chain of the PEO–PPO–PEO (P123) triblock copolymers. This additional chelating interaction would induce morphological change to the final SBA-15 products. From this point of view, it would be expected that in the presence of other metal cations, similar morphologies may

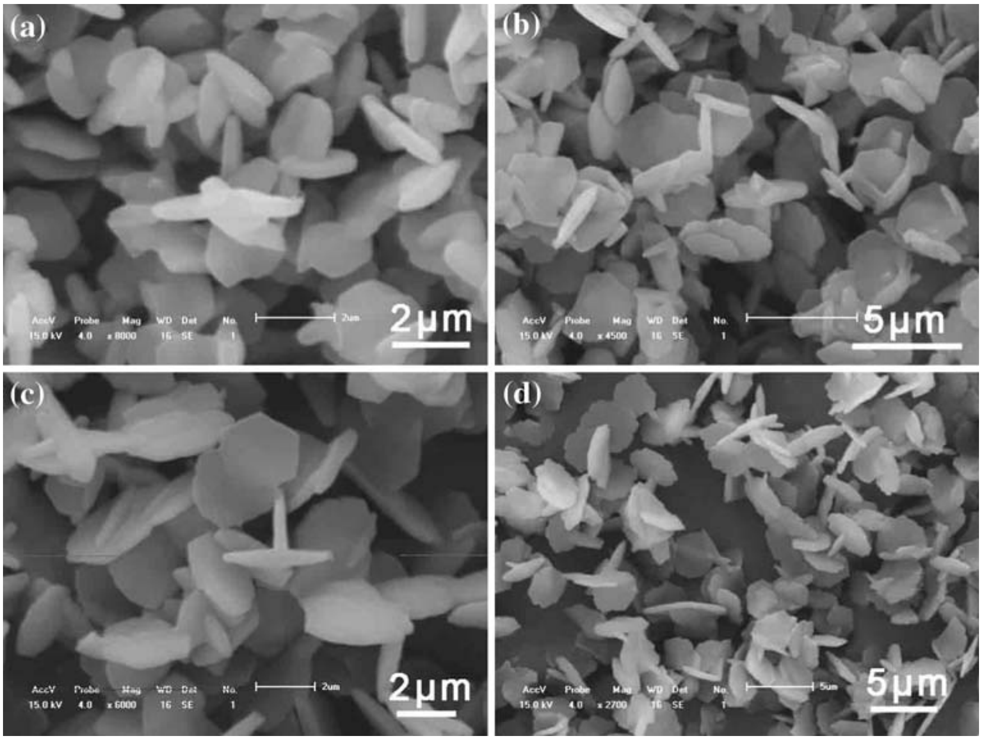

Fig. 4 SEM images of SBA-15 samples prepared under static condition at **a** 38 °C, **b** 60 °C, **c** 100 °C, **d** 130 °C

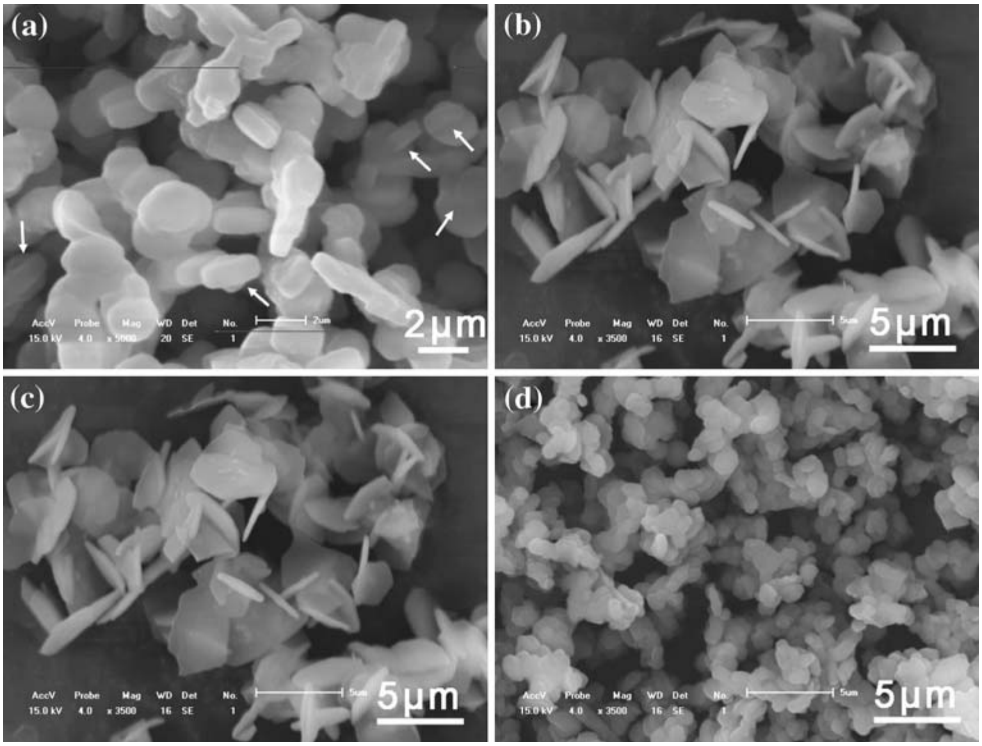

Fig. 5 SEM images of the as-synthesized products applied the Sn/Si radios of **a** 0:50, **b** 1:50, **c** 2:50, and **d** 5:50. The arrows indicate the cross-grown particles

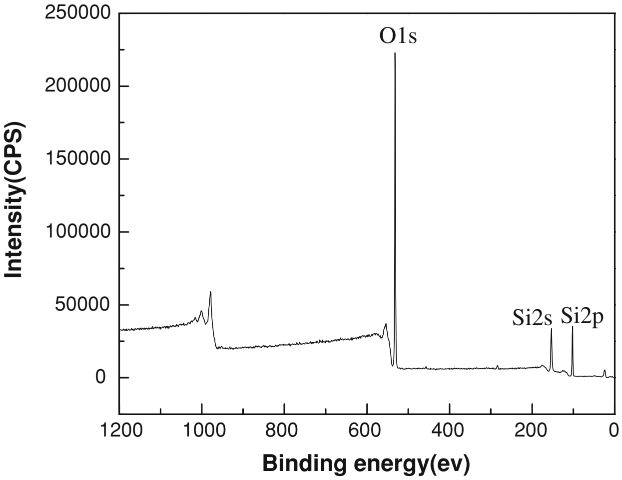

Fig. 6 XPS spectrum of the calcined SBA-15, and no signal of Sn can be detected

be obtained. In our experiments, when Mn^{2+} or Cu^{2+} ions was used in the synthesis, disc-like SBA-15 particles were obtained. However, their morphologies were neither regular nor uniform (Fig. 8). This proves that some type of specific interaction between metal cations and the copolymer also plays an important role in controlling the disc-like morphology of the product, although this interaction is not fully understood at this moment.

When the SBA-15 crossed-discs were used as hard templates, their carbon replicas were obtained (Fig. 9) according to the previously established method first developed by Ryoo and coworkers [19]. Figure 10 shows the nitrogen adsorption–desorption isotherm and PSD plots of the carbon discs. These monodispersed micro-mesoporous carbon crossed-discs have a pore volume of 0.80 $cm^3\ g^{-1}$, micropore area of 423 $m^2\ g^{-1}$, and total BET surface area of 1043 $m^2\ g^{-1}$. These carbon discs are expected to be useful in applications such as adsorbents, catalyst supports, electrode materials, and hydrogen storage.

Conclusion

In summary, we successfully synthesized mesoporous silica SBA-15 crossed-discs with short channels (200–350 nm in length) running parallel to the thickness of the discs. Based on the SEM and TEM observations, it is proposed that the cross-growth of the discs may start from the nucleation stage of SBA-15, and the presence of Sn^{2+}

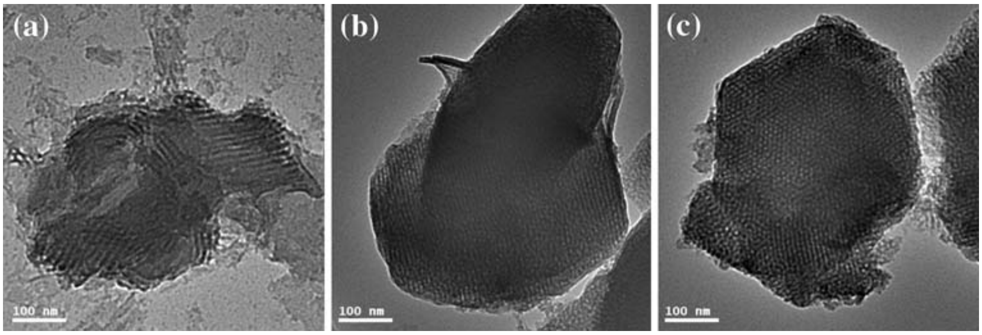

Fig. 7 TEM images of the products synthesized with Sn^{2+} and TMOS at 38 °C for **a** 12 min and **b**, **c** 40 min

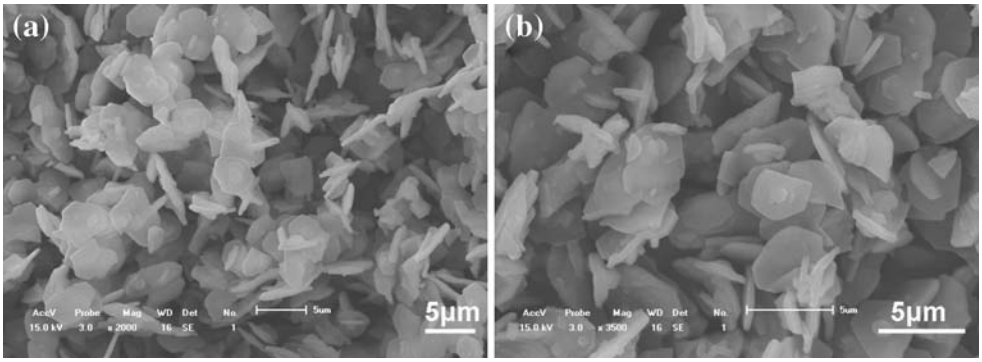

Fig. 8 SEM images of products prepared with addition of **a** Cu^{2+} and **b** Mn^{2+} cations

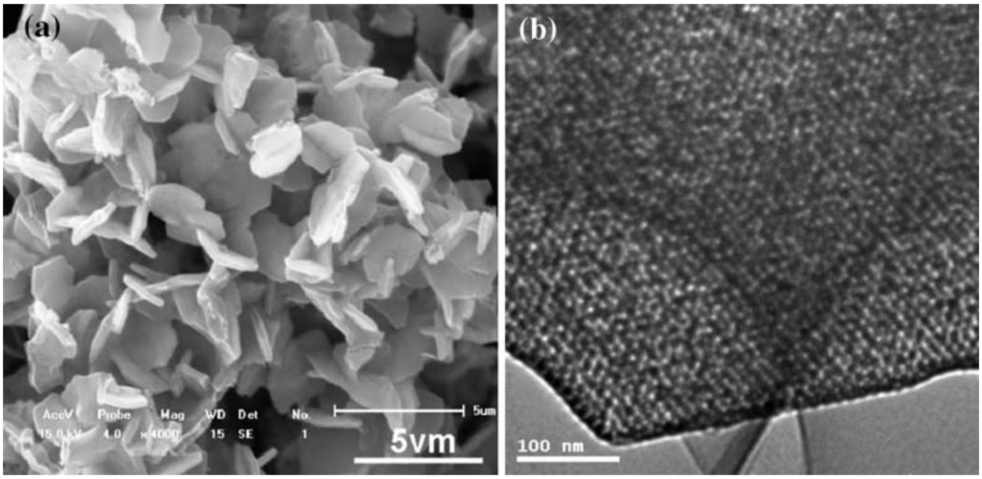

Fig. 9 **a** SEM image of the carbon crossed-discs, **b** the corresponding TEM image along the direction perpendicular to the disc surface

Fig. 10 The nitrogen adsorption–desorption isotherm (*left*) and pore size distribution (*right*) of the carbon replicas

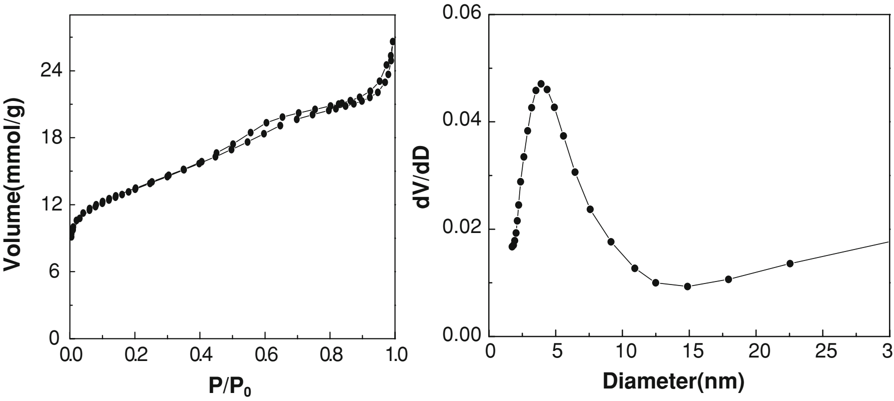

gives rise to a high aspect ratio of the crossed-discs. Carbon replicas were obtained using the SBA-15 crossed-discs as hard templates.

Acknowledgements This study was supported by the National Science Foundation of China (Grant No. 20873070), the National Basic Research Program of China (2009CB623502), and the NCET of Ministry of Education (NCET-07-0448).

References

1. Kresge CT, Leonowicz ME, Roth WJ, Vartuli JC, Beck JS (1992) Nature 359:710
2. Yang PD, Zhao D, Margolese DI, Chmelka BF, Stucky GD (1998) Nature 396:152
3. Yang P, Zhao D, Margolese DI, Chmelka BF, Stucky GD (1999) Chem Mater 11:2813
4. Zhao D, Feng J, Huo Q, Melosh N, Fredrickson GH, Chmelka BF, Stucky GD (1998) Science 279:548
5. Zhao D, Huo Q, Feng J, Chmelka BF, Stucky GD (1998) J Am Chem Soc 120:6024
6. Zhao D, Sun J, Li Q, Stucky GD (2000) Chem Mater 12:275
7. Sayari A, Han B, Yang Y (2004) J Am Chem Soc 126:14348
8. Linton P, Alfredsson V (2008) Chem Mater 20:2878
9. Kruk M, Cao L (2007) Langmuir 23:7247
10. Stevens W, Lebeau K, Mertens M, Van Tendeloo G, Cool P, Vansant EF (2006) J Phys Chem B 110:9183
11. Fahn YY, Su AC, Shen P (2005) Langmuir 21:431
12. Lu Q, Gao F, Komarneni S, Mallouk TE (2004) J Am Chem Soc 126:8650
13. Kosuge K, Sato T, Kikukawa N, Takemori M (2004) Chem Mater 16:899
14. Zhang H, Sun J, Ma D, Bao X, Klein-Hoffmann A, Weinberg G, Su D, Schlogl R (2004) J Am Chem Soc 126:7440
15. Sujandi PS, Han D, Han S, Jin M, Ohsuna T (2006) Chem Commun 4131
16. Kónya Z, Zhu J, Szegedi A, Kiricsi I, Alivisatos P, Somorjai GA (2003) Chem Commun 314
17. Chen S, Tang C, Chuang W, Lee J, Tsai Y, Chan J, Lin C, Liu Y, Cheng S (2008) Chem Mater 20:3906
18. Shan W, Wang B, Zhang Y, Tang Y (2005) Chem Comm 1877
19. Jun S, Joo SH, Ryoo R, Kruk M, Jaroniec M, Liu Z, Ohsuna T, Terasaki O (2000) J Am Chem Soc 122:10712
20. Yang W, Gao Y, Wu X, Yang Y, Huang G, Zhang Z, Chu P (2007) Appl Phys A 89:173
21. Yu C, Fan J, Tian B, Zhao D (2004) Chem Mater 16:889
22. Shah P, Ramaswamy AV, Ramaswamy V (2006) Chem Lett 35:860
23. Ruthstein S, Schmidt J, Kesselman E, Talmon Y, Goldfarb D (2006) J Am Chem Soc 128:3366